Electronic Supplementary Information

Aminoglycosides Antibiotics Bind to the Influenza A Virus RNA Promoter

Henna Kim[a], Mi-Kyung Lee[a], Junsang Ko[a], Chin-Ju Park[b], Meehyein Kim[c], Yujeong Jeong[a], Sungwoo Hong[a], Gabriele Varani[d], and Byong-Seok Choi[*a]

1. Materials and Methods

1.1 Fluorescence anisotropy measurement

Fluorescence anisotropy measurements were performed to determine the dissociation constants between aminoglycosides and influenza RNA promoter. RNA oligonucleotides were synthesized by Integrated DNA Technologies, Inc. and were annealed by heating to 95°C and slowly cooling to room temperature. Neomycin sulfate, paromomycin sulfate, kanamycin B sulfate, and tobramycin sulfate salt were purchased from Sigma Inc. and were used without further purification. 5-carboxytetramethylrhodamine succinimidyl ester was also purchased from Sigma Inc. and 5-carboxytetramethylrhodamine-labeled paromomycin (CRP) was prepared as previously described[1].

Fluorescence anisotropy experiments were carried out essentially in the same manner as published previously[2]. CRP concentration was determined by using a UV spectrophotometer at 550 nm using a molar extinction coefficient of $6.00 \times 10^4\ M^{-1}\ cm^{-1}$. Fluorescence anisotropy measurements were made on a Perkin-Elmer LS-55 luminescence spectrometer. The tracer solution containing 150 mM NaCl, 5 mM KCl, 1 mM $CaCl_2$, 1 mM $MgCl_2$, and 20 mM HEPES (pH 7.5) was excited at 550 nm and monitored at 580 nm. The slit widths used for excitation and emission were both 10 nm and the integration time was 5 s. Fifteen measurements were made for each data point and their average was used for calculation. The dissociation constant (K_d) for the interactions between influenza RNA promoter and CRP was determined by using the following equation[3]:

$$A = A_0 + \{\Delta A[RNA]_0 + [CRP]_0 + K_d - [([RNA]_0 + [CRP]_0 + K_d)^2 - 4[RNA]_0[CRP]_0]^{1/2}\} /2$$

where A and A_0 are fluorescence anisotropy of CRP in the presence and absence of RNA,

respectively, and ΔA is the difference between the fluorescence anisotropy of CRP in the presence of infinite concentration of RNA and the fluorescence anisotropy in the absence of RNA. $[RNA]_0$ and $[CRP]_0$ are the initial concentrations of RNA and CRP, respectively.

In the competitive binding assay with other aminoglycosides, the following equation was used to determine the dissociation constant (K_D) for the interactions between influenza RNA promoter and aminoglycosides[4]:

$$A= A_\infty + (A_\infty - A_0)/[K_d([\text{aminoglycoside}]+K_D)/(K_D[RNA])+1]$$

where A_∞ is the fluorescence anisotropy in the presence of an infinite concentration of RNA and K_d is the dissociation constant for the interactions between the influenza RNA promoter and CRP determined from the previous equation. Both K_d and K_D values were averaged from three independent experiments.

1.2 RNA sample preparation

Template DNAs were purchased from Integrated DNA Technologies, Inc. and used without further purification. RNA oligonucleotides were synthesized by *in vitro* transcription using annealed DNA template, T7 promoter DNA, 5 mM NTP, 8% PEG 8000, and T7 RNA polymerase. The $MgCl_2$ concentrations were varied in order to optimize the transcription condition. The transcribed RNA was precipitated by ethanol precipitation and then purified by denaturing gel electrophoresis (20% (w/w) acrylamide/bisacrylamide (19:1), 7 M urea). The gel band was excised and eluted by electroelution into 1X TBE. The RNA was exchanged into autoclaved deionized water and lyophilized. The pellet was dissolved in NMR buffer containing 10 mM sodium phosphate (pH 6.0), 50 mM NaCl, and 0.1 mM EDTA.

1.3 NMR spectroscopy

NMR spectra were acquired at 600 MHz using a Varian Unity Inova spectrometer. The spectra were processed with NMR-Pipe and Varian VNMR software. All of the spectra were analyzed with SPARKY (University of California, San Francisco). In order to map the binding site of the aminoglycoside, 1D titration experiment with increasing amounts of aminoglycoside was performed at 277 K. The buffer for the NMR experiment contained 10 mM potassium phosphate (pH 6.0), 50 mM NaCl and 0.1 mM EDTA.

RDC-based homology modeling

The RDCs were measured for the ^{13}C-labeled vRNA complexed with neomycin in liquid crystalline medium containing 25 mg/mL of filamentous phage Pf1 at 298K. The buffer contained 10 mM potassium phosphate (pH 6.0), 50 mM NaCl, and 0.1 mM EDTA. ^{1}H-^{13}C RDCs were measured in 2D ^{13}C/^{1}H IPAP-HSQC experiments. XPLOR-NIH was used for refinement based on protocols from the previous research[5]. The lowest energy structure among 20 converged structures was analyzed by PALES[6]. The experimental ^{1}H-^{13}C RDC values are well correlated to the back-calculated RDCs with correlation coefficient of 0.912. The optimal axial alignment tensor (Da) and the rhombicity were -5.23Hz and 0.32, respectively. The figures were generated using PyMOL[7].

Docking structure calculations

CNS-type topology and parameter files of neomycin B were created from the PRODRG[8] online server. HADDOCK 2.1 was used to generate the complex structure between vRNA and neomycin using the initial rigid-body docking and semi-flexible simulated annealing procedure.

Intermolecular NOEs obtained from NOESY spectra were used for ambiguous interaction restraints (AIR) and strong seven intermolecular NOEs were translated into unambiguous distance restraints. Ten structures with the lowest energy and RMSD were analyzed by HADDOCK software.

1.4 RNA constructs used for K_d measurement

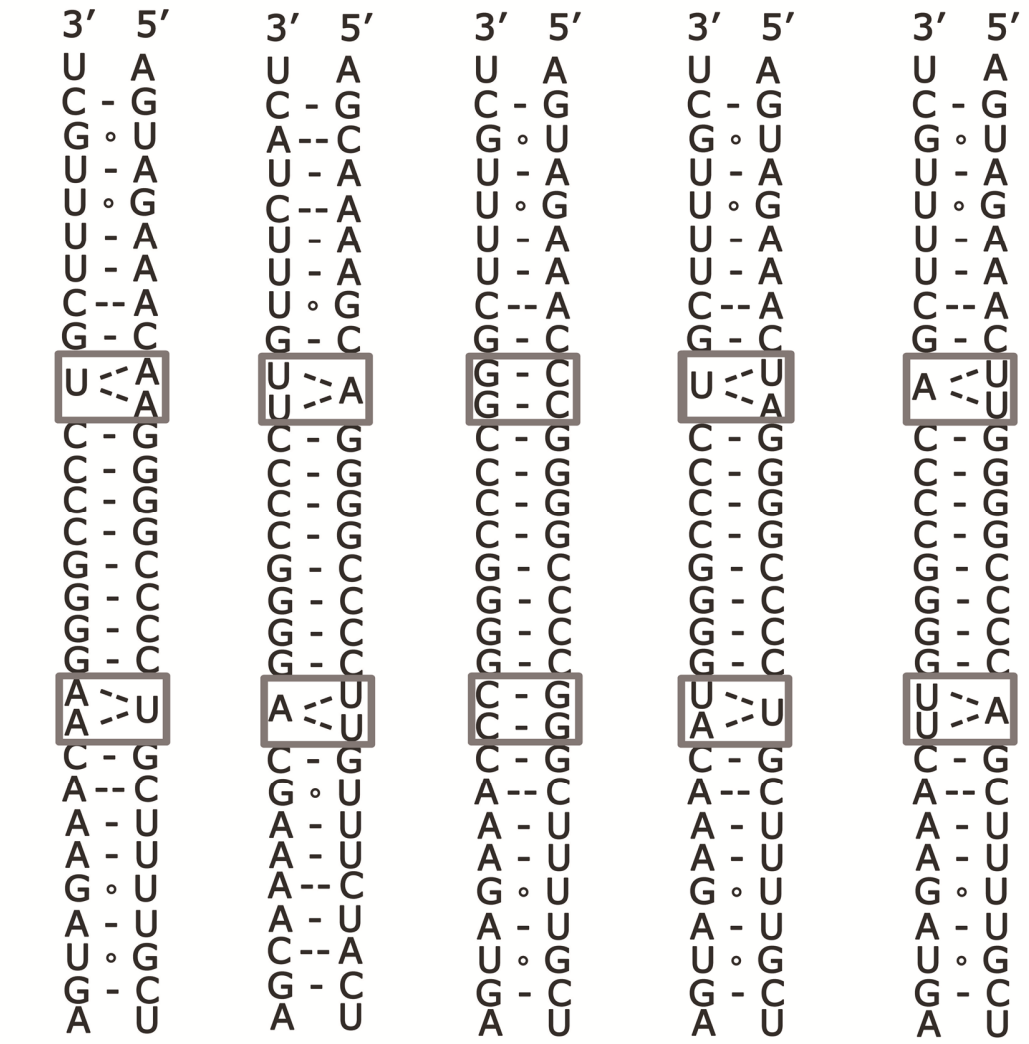

Fig. S1 RNA constructs used for K_d measurement (A) vRNA; (B) cRNA; (C) no loop G-C; (D) (U·A)-U; (E) cRNA loop

2. Supporting Results

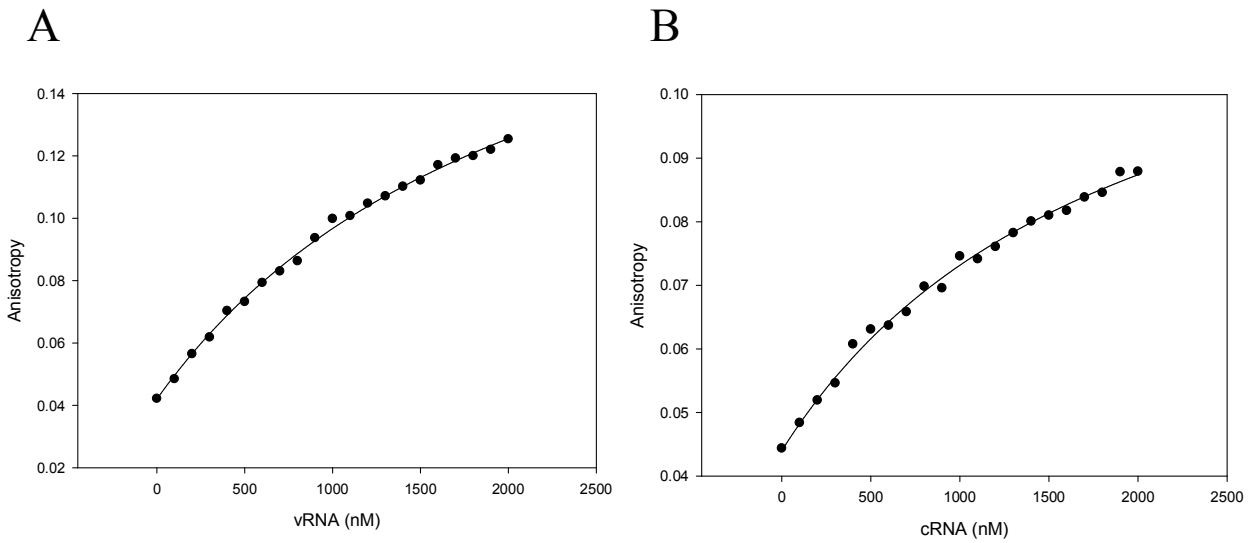

Fig. S2 Fluorescence anisotropy of the CRP as a function of (A) vRNA concentration and (B) cRNA concentration

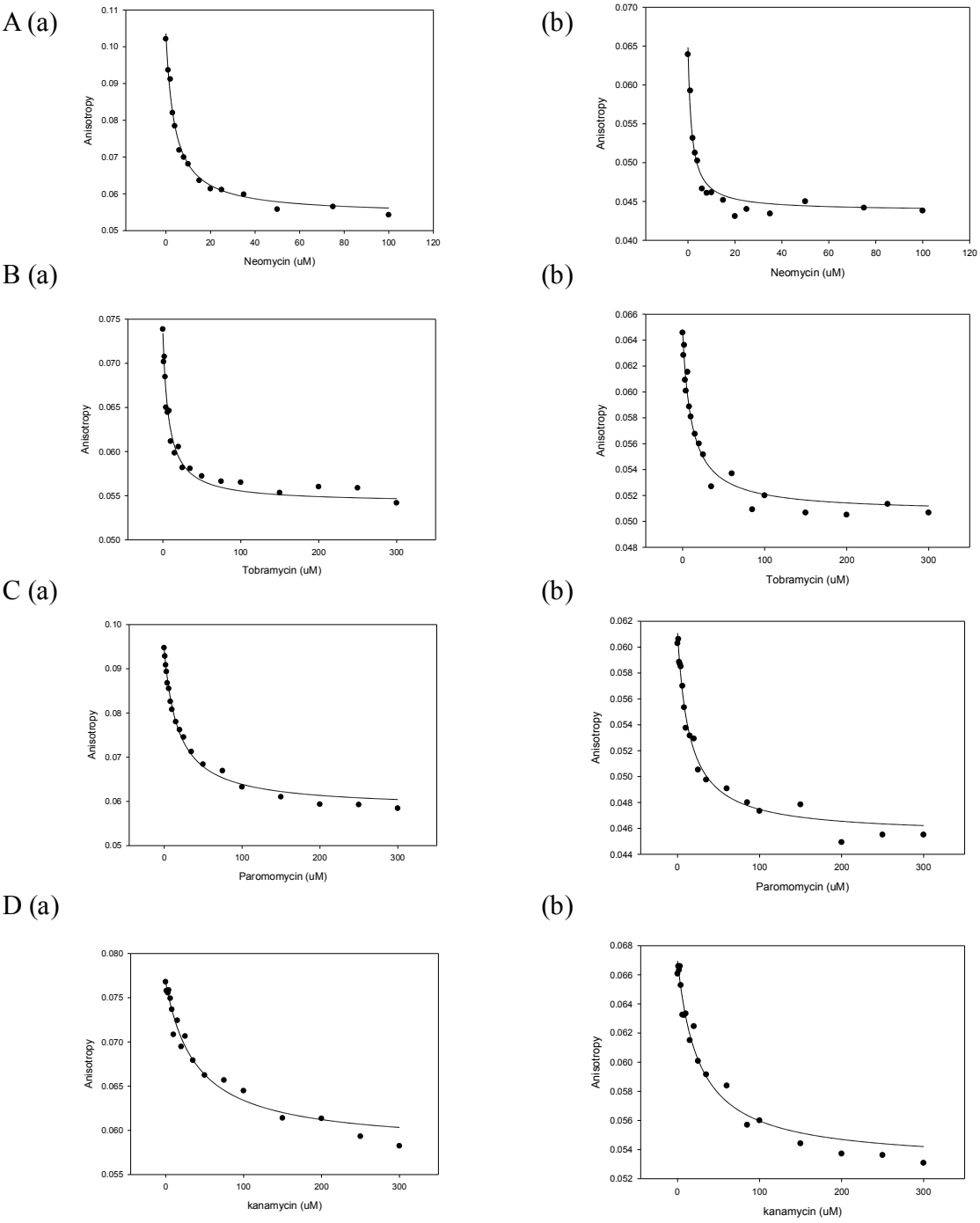

Fig. S3 Fluorescence anisotropy of CRP (20 nM) solution containing (a) vRNA (1 μM) and (b) cRNA (1 μM), as a function of (A) neomycin, (B) tobramycin, (C) paromomycin and (D) kanamycin concentrations

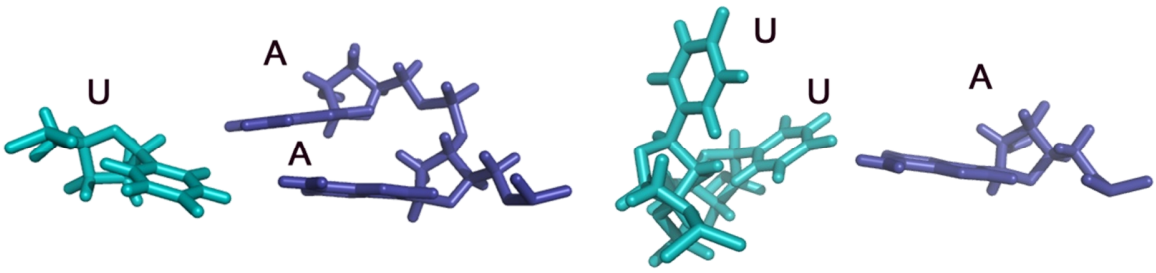

Fig. S4 Comparison of internal loop structure of vRNA (Left, PDB ID: 1JO7) and cRNA (Right, PDB ID: 1M82)

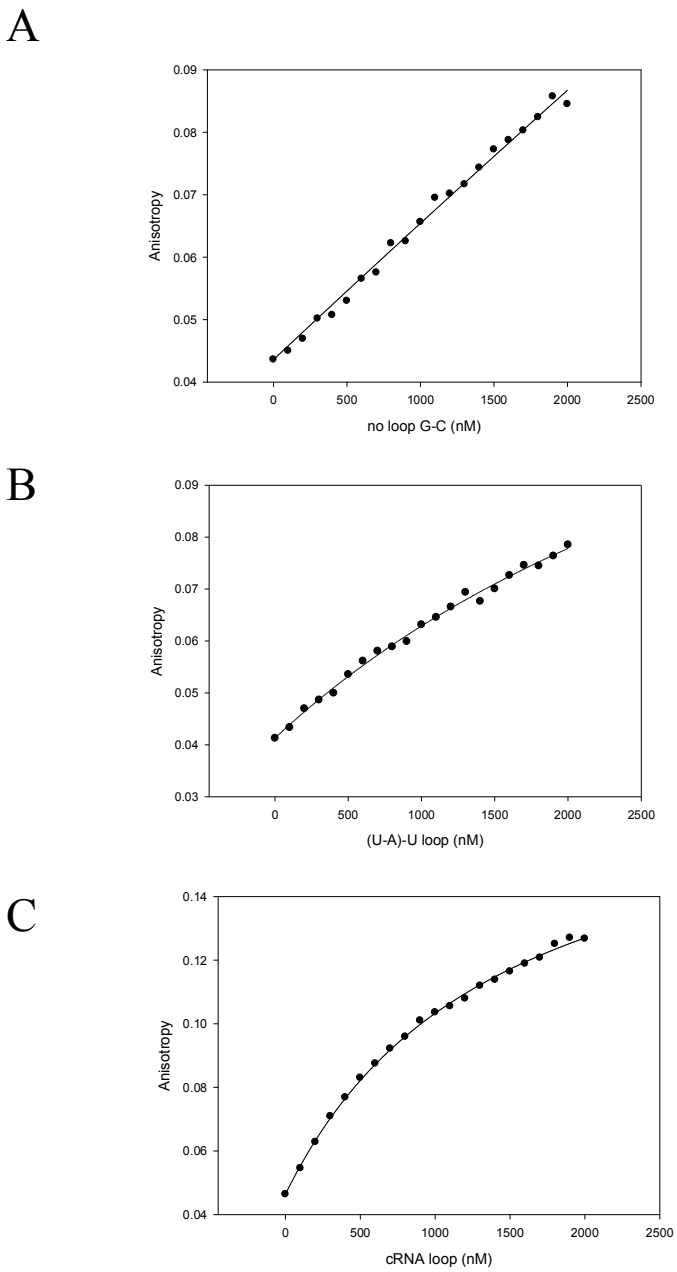

Fig. S5 Fluorescence anisotropy of CRP (20 nM) as a function of RNA concentration for (A) no loop G-C, (B) (U·A)-U loop, and (C) cRNA loop

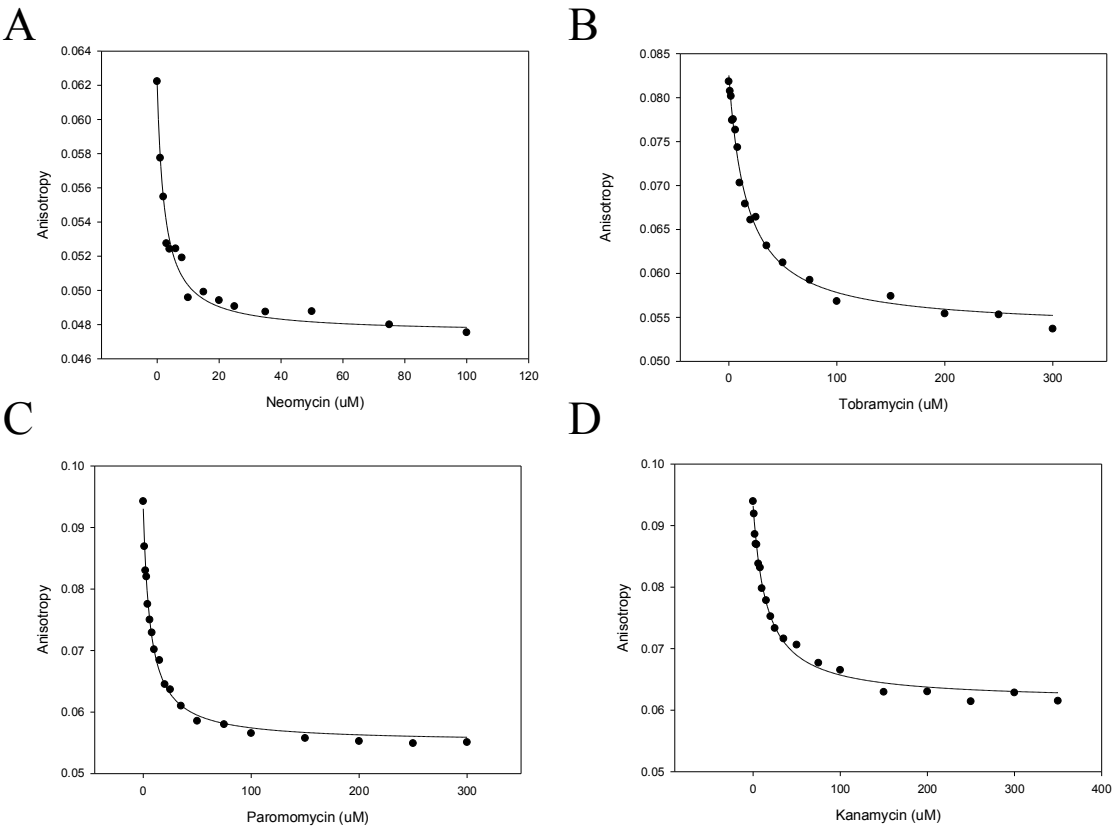

Fig. S6 Fluorescence anisotropy of CRP (20 nM) solution containing the (U·A)-U mutant RNA (1 μM) and as a function of (A) neomycin, (B) tobramycin, (C) paromomycin, and (D) kanamycin concentrations

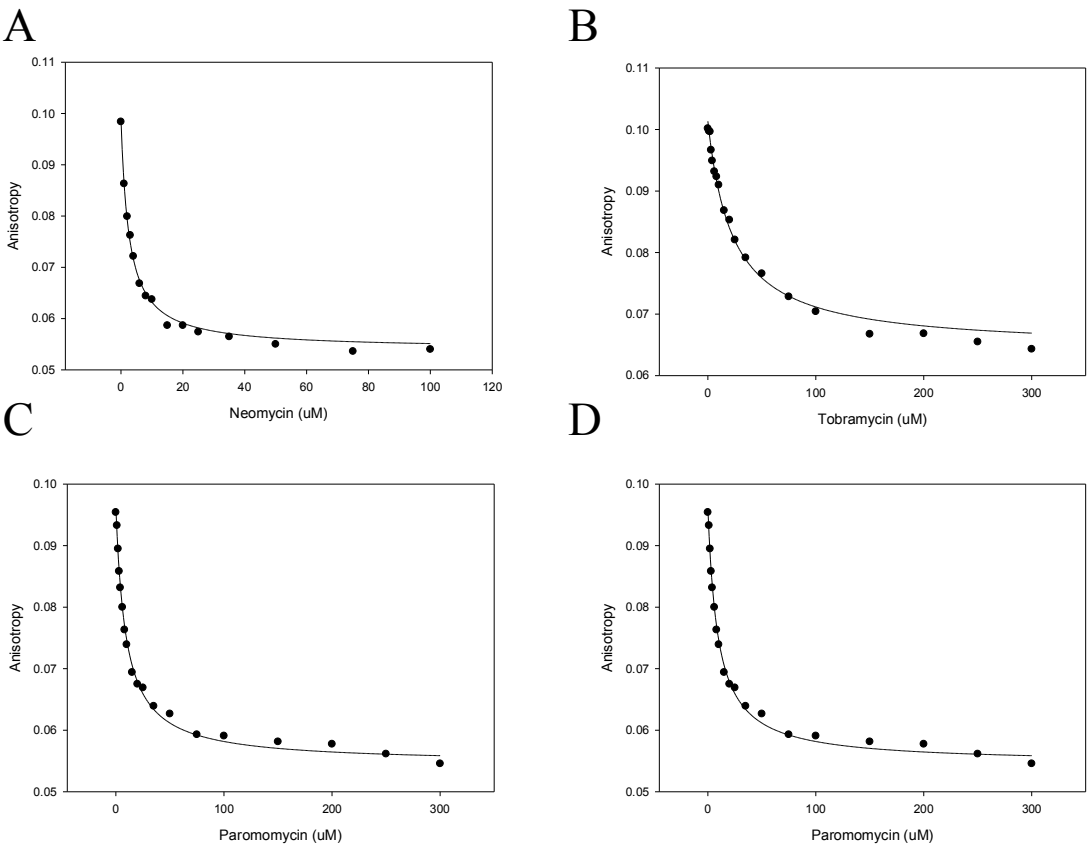

Fig. S7 Fluorescence anisotropy of CRP (20 nM) solution containing the cRNA loop mutant RNA (1 μM) and as a function of (A) neomycin, (B) tobramycin, (C) paromomycin, and (D) kanamycin concentrations

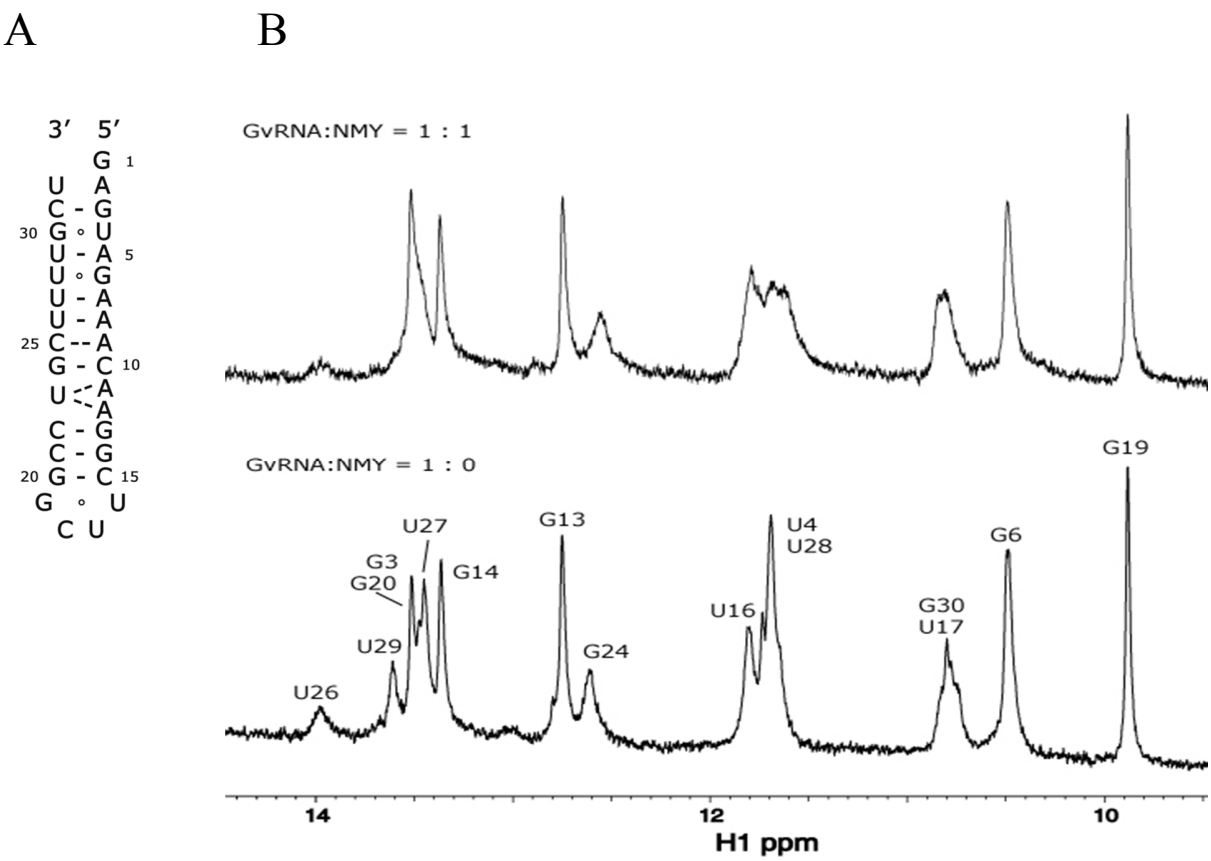

Fig. S8 1D ^{1}H-NMR titration of vRNA with neomycin B (A) Secondary structure of vRNA (B) Imino proton NMR spectra of free vRNA (bottom) and vRNA on addition of one equivalent of neomycin B (NMY) (top)

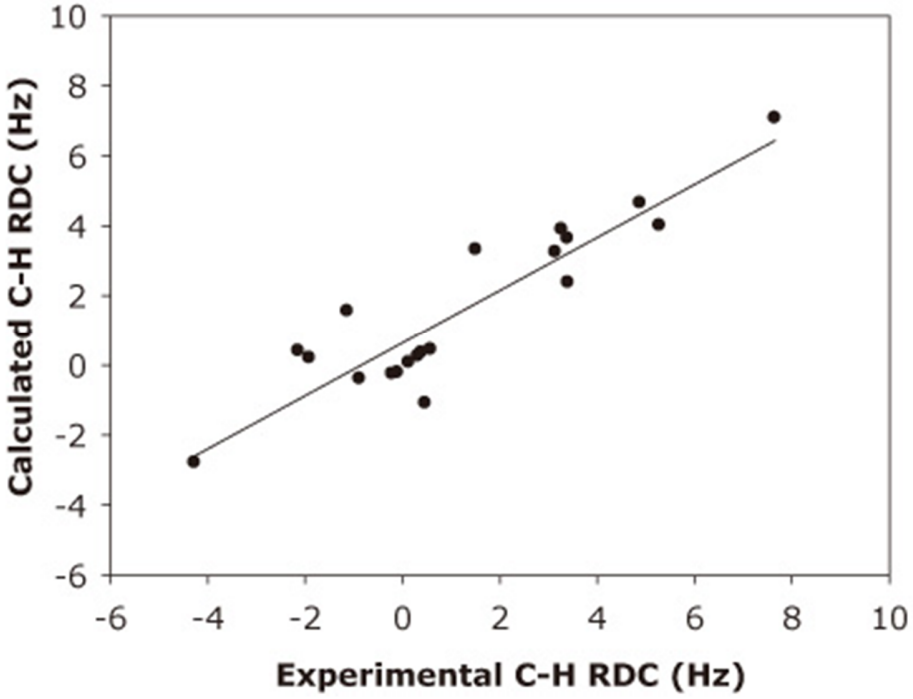

Fig. S9 RDC fit. Experimental ^{13}C-^{1}H RDC values were plotted against calculated values for the complex between vRNA and neomycin

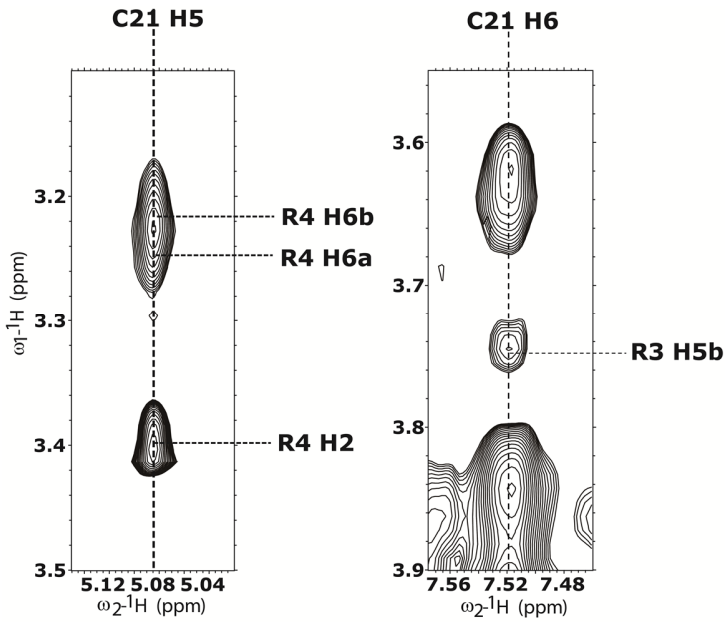

Fig. S10 Regions of 2D ^{1}H- ^{1}H NOESY spectra showing intermolecular NOEs between vRNA and neomycin B

Fig. S11 Overlay of the free vRNA (PDB ID: 1JO7) (cyan) and the complex of vRNA with neomycin (purple).

Table S1. ^{13}C-^{1}H RDCs observed for the neomycin-vRNA complex

Residue Number	Residue type	Heteroatom	Proton	RDC, Hz
1	GUA	C8	H8	7.94
2	ADE	C2	H2	-0.1
4	URI	C5	H5	-0.87
5	ADE	C2	H2	-2.14
5	ADE	C8	H8	0.13
6	GUA	C8	H8	-0.21
7	ADE	C2	H2	0.13
7	ADE	C8	H8	-4.65
8	ADE	C8	H8	-0.5
9	ADE	C2	H2	3.39
10	CYT	C6	H6	0.07
11	ADE	C2	H2	3.52
11	ADE	C8	H8	4.88
12	ADE	C2	H2	-0.75
15	CYT	C5	H5	0.32
15	CYT	C6	H6	-4.9
16	URI	C5	H5	4.92
16	URI	C6	H6	-1.76
17	URI	C5	H5	0.38
17	URI	C6	H6	2.51
18	CYT	C5	H5	0.63
18	CYT	C6	H6	0.07
19	GUA	C8	H8	0.5
20	GUA	C8	H8	0.39
21	CYT	C5	H5	5.9
22	CYT	C5	H5	5.28
22	CYT	C6	H6	-1.91
24	GUA	C8	H8	3.27
25	CYT	C6	H6	-1.81
26	URI	C5	H5	-1.26
28	URI	C5	H5	7.65
28	CYT	C6	H6	3.4
29	URI	C5	H5	-2.01
29	URI	C6	H6	-0.88
30	GUA	C8	H8	0.58

31	GUA	C6	H6	-15.21
2	ADE	C1’	H1’	-0.5
3	GUA	C1’	H1’	1.01
5	ADE	C1’	H1’	0.88
6	GUA	C1’	H1’	2.05
7	ADE	C1’	H1’	-4.27
8	ADE	C1’	H1’	8.79
10	CYT	C1’	H1’	7.32
13	GUA	C1’	H1’	1.51
14	GUA	C1’	H1’	0.56
16	URI	C1’	H1’	0.13
17	URI	C1’	H1’	0.38
18	CYT	C1’	H1’	-0.25
19	GUA	C1’	H1’	-0.38
21	CYT	C1’	H1’	0.25
22	CYT	C1’	H1’	-0.13
29	URI	C1’	H1’	3.14
30	GUA	C1’	H1’	-1.13
31	CYT	C1’	H1’	0.47
32	URI	C1’	H1’	-0.63

3. References

1. Y. Wang, K. Hamasaki and R. R. Rando, *Biochemistry*, 1997, **36**, 768-779.
2. D. H. Ryu and R. R. Rando, *Bioorg Med Chem*, 2001, **9**, 2601-2608.
3. Y. Wang and R. R. Rando, *Chem Biol*, 1995, **2**, 281-290.
4. J. B. Marchand, D. A. Kaiser, T. D. Pollard and H. N. Higgs, *Nat Cell Biol*, 2001, **3**, 76-82.
5. J. J. Chou, S. Li and A. Bax, *J Biomol NMR*, 2000, **18**, 217-227.
6. M. Zweckstetter, *Nature protocols*, 2008, **3**, 679-690.
7. Schrodinger, LLC, 2010.
8. A. W. Schuttelkopf and D. M. van Aalten, *Acta crystallographica. Section D, Biological crystallography*, 2004, **60**, 1355-1363.